

Numerical model to predict microstructure of the heat treated of steel elements

T. Domański^{*a}, A. Bokota^b

Institute of Mechanics and Machine Design^a, Institute of Computer and Information Sciences^b
Czestochowa University of Technology 42-200 Czestochowa, 73 Dąbrowskiego str., Poland

*Corresponding author: e-mail: domanski@imipkm.pcz.czest.pl

Received 11.04.2011; Approved for print on: 26.04.2011

Abstract

In work the presented numerical models of tool steel hardening processes take into account thermal phenomena and phase transformations. Numerical algorithm of thermal phenomena was based on the Finite Elements Methods of the heat transfer equations. In the model of phase transformations, in simulations heating process continuous heating (CHT) was applied, whereas in cooling process continuous cooling (CCT) of the steel at issue. The phase fraction transformed (austenite) during heating and fractions during cooling of ferrite, pearlite or bainite are determined by Johnson-Mehl-Avrami formulas. The nascent fraction of martensite is determined by Koistinen and Marburger formula or modified Koistinen and Marburger formula. In the simulations of hardening was subject the fang lathe of cone (axisymmetrical object) made of tool steel.

Keywords: Hardening, phase transformations, numerical simulations

1. Introduction

Thermal treatment including hardening is a complex technological process aiming to obtain high hardness, high abrasion resistance, high durability of the elements hardened as well as suitable initial structure to be used in the subsequent thermal treatment processes as a result of which the optimum mechanical properties of the elements are received.

Today an intense development of numerical methods supporting designing or improvement of already existing technological processes are observed. The technologies mentioned above include also steel thermal processing comprising hardening. Efforts involving thermal processing numerical models aim to encompass an increasing number of input parameters of such a process [1-4].

Predicting of final properties of the element undergoing hardening is possible after determination of the type and features of the microstructure to be created, accompanying such technology of product quality improvement. For this to be achieved, it is necessary to take into account, first of all, thermal

phenomena and phase transitions in the numerical model [1,5,8].

As a consequence of analyzing of the thermal processing results many mathematical and numerical models were obtained [1,3,6-8]. A basic element of almost all studies regarding transformations of austenite into ferrite, pearlite and bainite is the Avrami equation with respect of the TTT diagram-based models and the general Kolmogorov Johnson-Mehl-Avrami equation with respect to the models using classical nucleation theory [2-6]. The Koistinen and Marburger's equation is, on the other hand, fundamental equation enabling prediction of the kinetics of the martensite transformation [1-6]. The results of the numerical simulations of the phenomena mentioned above are dependent on the precision in calculation of the instantaneous temperature and solid-state phase kinetics, the latter significantly affecting and the microstructure final. Therefore accuracy of the solid-state phase transformations model for each steel grade is very important here.

Phase transformations numerical models exploiting isothermal heating and cooling curves can be applied with respect to several carbon steel grades if the isothermal heating and cooling curves are adequately moved. However, the values of the curve move should be confirmed by the results of experimental research

conducted for this specific or a similar steel grade. Application of TTT diagrams facilitates parallel calculations and thus it is easier to take the heat of the phase transformations into account in the numerical algorithm [1,6]. On the other hand, CCT diagrams enable more precise determination of fractions and kinetics of the phases depending of the cooling rate [2,5,7].

The choice of suitable model can be dependent on kinds of lead hardening simulations. It can be by parallel simulation of thermal phenomena, phase transformations and mechanical phenomena (Fig. 1), or series block simulations – thermal block, phase transformations, and then mechanical phenomena block [5].

Models using diagrams of isothermal heating and cooling can be applied both with respect to parallel and block sequential simulation since the transformations starting and ending times are determined at the crossing of the starting and ending curves of the transformations carried out at a fixed temperature [1-5].

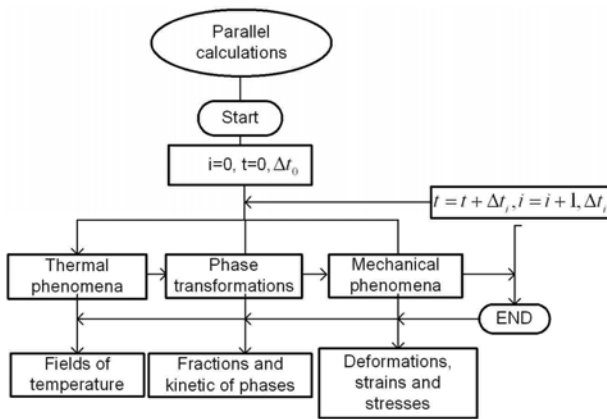


Fig. 1. Diagram of parallel hardening simulation

Models using continuous heating and cooling diagrams can be directly applied only in a block sequential simulation. In this case transformation starting and ending times are determined at the crossing of the starting and ending curves of the transformations and the heating or cooling temperature curves. In the parallel simulation model the transformation starting time is directly determined at the crossing of the transformations starting curve and heating or cooling temperature curves whereas the transformation ending time can be established using the technique of temperature curve approximation within the expected range of the transformation.

In the study the CCT diagram-based models are proposed [5,9].

Accuracy of the proposed tool steel hardening methods was proved by comparing the results of numerical simulations and experimental research results presented in the studies [5].

2. Temperature fields

Temperature field are obtain with solved of transient heat equation (Fourier equation) with source unit:

$$\nabla \cdot (\lambda \nabla(T)) - C \frac{\partial T}{\partial t} = -Q^v \quad (1)$$

where: $\lambda = \lambda(T)$ is the heat conductivity coefficient, $C = C(T)$ is effective heat coefficient, Q^v is intensity of internal source (this can also be the phase transformations heat).

Superficial heating investigation in model by boundary conditions Neumann (heat flux q_n), however cooling are modelling by boundary conditions Newton with depend on temperature coefficient of heat transfer:

$$-\lambda \frac{\partial T}{\partial n} \Big|_{\Gamma} = q_n = \alpha^T(T) (T|_{\Gamma} - T_{\infty}) \quad (2)$$

In heating simulation on surfaces except heating source, also radiation through overall heat transfer coefficient was taken into account:

$$-\lambda \frac{\partial T}{\partial n} \Big|_{\Gamma} = q_n = \alpha_0 \sqrt[3]{T|_{\Gamma} - T_{\infty}} (T|_{\Gamma} - T_{\infty}) = \alpha^*(T|_{\Gamma} - T_{\infty}) \quad (3)$$

where: $\alpha^T(T)$ is heat transfer coefficient, α_0 is heat transfer coefficient experimental determine, Γ is surface, from which is transfer heat, T_{∞} is temperature of medium cooling.

As it mention, the problem solved by FEM.

3. Phase transformations

In the model of phase transformations take advantage of diagrams of continuous heating (CHT) and cooling (CCT) [5,9].

In both case the phase fractions transformed during continuous heating (austenite) is calculated using the Johnson-Mehl and Avrami formula (4) or modified Koistinen and Marburger formula (in relations on rate of heating) (5) [1-7]:

$$\underline{\eta}_A(T, t) = 1 - \exp(-b(t_s, t_f) (t(T))^n) \quad (4)$$

$$\underline{\eta}_A(T, t) = 1 - \exp\left(-\ln(\eta_s) \frac{T_{sA} - T}{T_{sA} - T_{fA}}\right), \dot{T} \geq 100 \text{ K/s} \quad (5)$$

where: $\underline{\eta}_A$ is austenite initial fraction nescient in heating process, T_{sA} is temperature of initial phase in austenite, T_{fA} – is final temperature this phase.

The coefficient $b(t_s, t_f)$ and $n(t_s, t_f)$ are obtain with (4) next assumption of initial fraction ($\eta_s = 0.01$) and final fraction ($\eta_f = 0.99$) and calculation are by formulas:

$$n(t_s, t_f) = \frac{\ln(\ln(0.01)/\ln(0.99))}{\ln(t_f/t_s)}, \quad b(t_s, t_f) = \frac{-\ln(0.99)}{(t_s)^n} \quad (6)$$

Pearlite and bainite fraction (in the model of phase transformations upper and lower bainite is not distinguish) are determine by Johnson-Mehl and Avrami formula.

$$\eta_i(T, t) = \chi \left(1 - \exp(-b(t(T))^n) \right) \quad (7)$$

The nascent fraction of martensite is calculated using the Koistinen and Marburger formula [2,3].

$$\eta_M(T) = \chi \left(1 - \exp \left(\ln(0.01) \frac{M_s - T}{M_s - M_f} \right) \right) \quad (8)$$

or modified Koistinen and Marburger formula [3,4,7]:

$$\eta_M(T) = \chi \left(1 - \exp \left(- \left(\frac{M_s - T}{M_s - M_f} \right)^m \right) \right) \quad (9)$$

where

$$\chi = \eta_{()}^{\%} \underline{\eta}_A \text{ for } \underline{\eta}_A \geq \eta_{()}^{\%} \text{ and } \chi = \underline{\eta}_A \text{ for } \underline{\eta}_A < \eta_{()}^{\%} \quad (10)$$

$\eta_{()}^{\%}$ is the maximum phase fraction for the established of the cooling rate, estimated on the ground of the continuous cooling graph, m is the constant chosen by means of experiment. For considered steel determine, that $m = 3.3$ if the start temperature of martensite transformations is equal $M_s = 493$ K, and end this transformations is in temperature $M_f = 173$ K [5,9].

Increases of the isotropic deformation caused by changes of the temperature and phase transformation in the heating and cooling processes are calculated using the following relations:

- heating

$$d\varepsilon^{Tph} = \sum_{\alpha=1}^{\alpha=5} \alpha_{\alpha} \eta_{\alpha} dT - \varepsilon_A^{ph} d\eta_A \quad (11)$$

- cooling

$$d\varepsilon^{Tph} = \sum_{\alpha=1}^{\alpha=5} \alpha_{\alpha} \eta_{\alpha} dT + \sum_{\beta=2}^{\beta=5} \varepsilon_{\beta}^{ph} d\eta_{\beta} \quad (12)$$

where: $\alpha_{\alpha} = \alpha_{\alpha}(T)$, are coefficients of thermal expansion of: austenite, bainite, ferrite, martensite and pearlite, respectively, ε_A^{ph} is the isotropic deformation accompanying transformation of the input structure into austenite, whereas $\varepsilon_{\beta}^{ph} = \varepsilon_{\beta}^{ph}(T)$ are isotropic deformations from phase transformation of: austenite into bainite, ferrite, martensite, or of austenite into pearlite, respectively. These values are usually adopted on the basis of experimental research conducted on a heat cycle simulator [5].

Heat of phase transformations take into account in source unit of conductivity equation (1) calculate by formula:

$$Q^v = \sum_k H_k^{\eta_k} \dot{\eta}_k \quad (13)$$

where: $H_k^{\eta_k}$ is volumetric heat k - phase transformations, $\dot{\eta}_k$ is rate of change fractions k - phase [10,11].

The methods for calculation of the fractions of the phases created referred to above were used for carbon tool steel represented by C80U steel. CCT diagrams for this steel grade are presented in the figures 2 and 3.

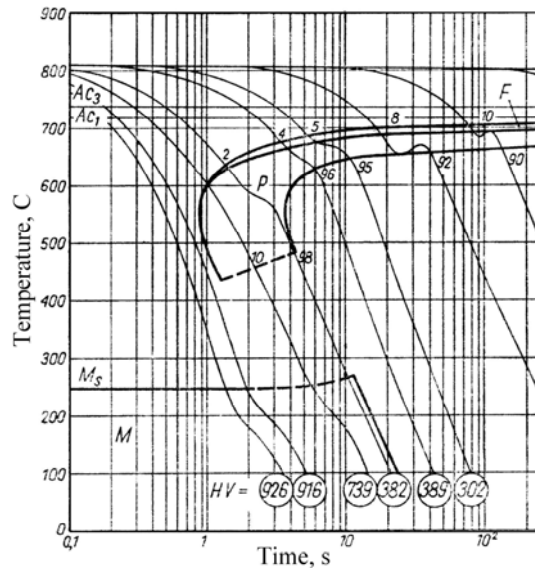


Fig. 2. Diagram CCT for steel C80U [9]

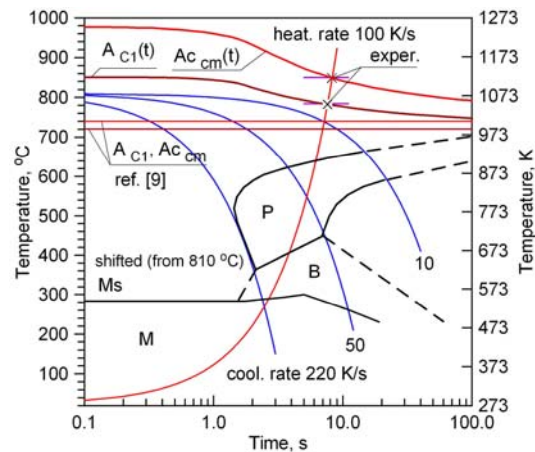


Fig. 3. Shifted diagram CCT with CHT curves for considered steel [5]

After analysing of the above diagrams it can be noticed that steel under consideration does not contain ferrite but can contain remnant cementite [5] (Figs 2,3).

The curves of CCT diagrams are introduced into a relevant module of phase fraction determination with supplementary information regarding maximum participation of each phase. However, in the model based upon the diagrams of continuous cooling relevant ranges determine the paces of cooling evaluated

to the time when the temperature achieves the transformation starting curve.

In the parallel simulation model the transformation starting time is directly determined at the crossing of the transformations starting curve and the heating or cooling temperature curves whereas the transformation ending time can be established using the technique of temperature curve approximation within the expected range of the transformation (Fig. 4).

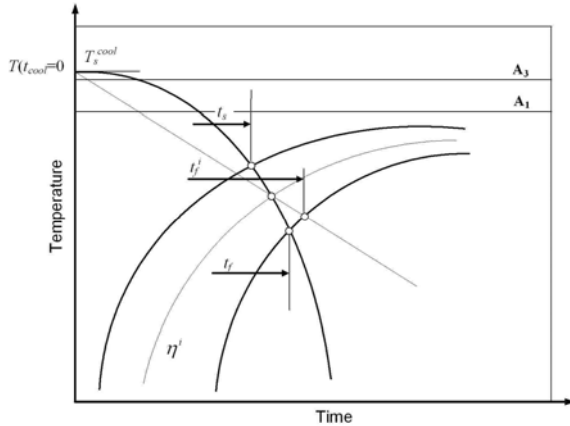


Fig. 4. Determination of time t_f in the parallel simulation (curve CCT, cooling)

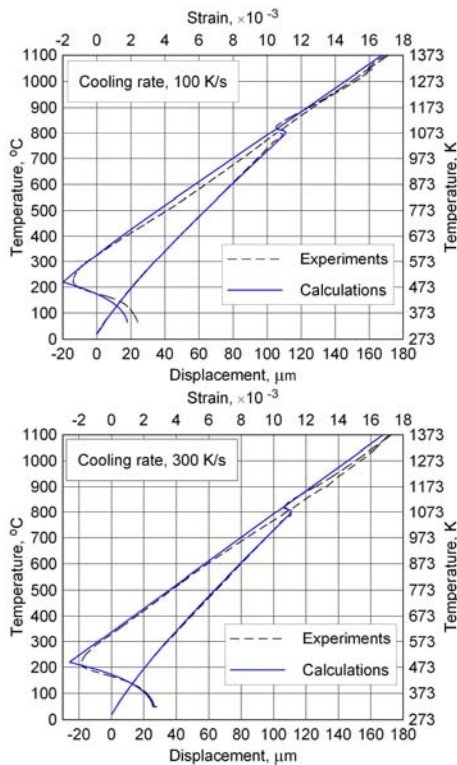


Fig. 5. Experimental and simulating dilatometric curves

In order to confirm the accuracy of the phase transformation model dilatometric tests were carried out on the samples of the steel under consideration. The tests were conducted at the Institute for Ferrous Metallurgy in Gliwice. The model was verified by comparing the dilatometric curves received for different cooling rates with simulation curves. On the basis of the analysis of the results a slight move of CCT diagram was made in order to reconcile the initiation time of the simulation transformation and the times obtained in the experimental research (Fig. 3). These moves were presented, for example, in the studies [5].

On the basis of the analysis of simulation and dilatometric curves the values of the thermal expansion coefficient ($\alpha_{(i)}$) and isotropic structural deformations of each structural component were specified. These coefficients are: 22, 10, 10 and 14.5 ($\times 10^{-6}$) [1/K] and 0.9, 4.0, 8.5 and 1.9 ($\times 10^{-3}$). It was adopted that 1,2,3,4 and 5 refer to austenite, bainite, martensite and pearlite, respectively [5].

Exemplary comparisons of the simulation and experiment results are displayed in the figure 5. The transformation kinetics corresponding to the established speeds of cooling was presented in the figure 6.

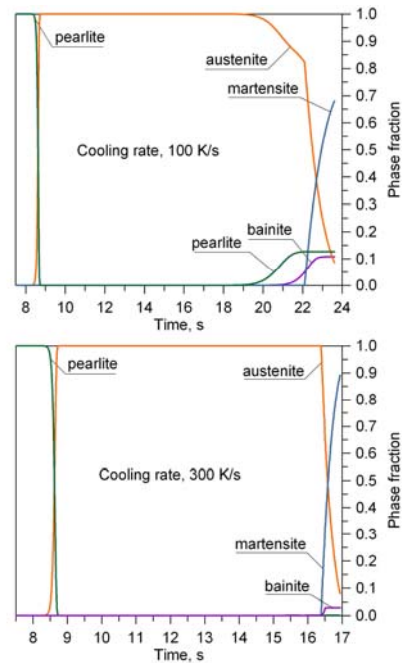


Fig. 6. Kinetics of phases for the fixed rates cooling

Coefficient of thermal expansion the pearlite structure for considered steel is dependent on temperature (Fig. 5), approximate this coefficient by square function [5].

Analysing results from the model notice, that advantageous is use in modelling of phase transformations the CCT graph for considered group steel. Accuracy results, particularly in range rate cooling are obtain, in which forming also bainite (Fig. 6b).

4. Example of hardening elements of machines

As it has been already mentioned, the simulations of hardening were subject the fang lathe of cone (axisymmetrical object) made of tool steel. The shape and dimensions considered object was presented on the figure 7.

The superficial heating (surface hardening) the section of side surface of cone was modelling Neumann boundary conditions taken Gauss distributions of heating source:

$$q_n = \frac{Q}{2\pi r^2} \exp\left(-\frac{(z-h)^2}{2r^2 \cos^2 \alpha}\right) \quad (14)$$

The peak value of heating source established on $Q=3500$ W, radius $r=15$ mm, angle $\alpha=30^\circ$ (Fig. 10). The cooling of boundary contact with air was modelled boundary conditions (3) taking $\alpha_0=30$ W/(m²K) [4,9,22]. The initial structure was pearlite. The thermophysical values occurrence in conductivity equations (λ, C) was taken constant, averages values from passed in work data [1,3,4] suitable assumed: 35 [W/(mK)], 5.0×10^6 [J/(m³K)]. The heat of phase transformations was assumed on the work [4,20]: $H_{A-P}=800 \times 10^6$, $H_{A-B}=314 \times 10^6$, $H_{A-M}=630 \times 10^6$ [J/(m³K)]. The initial temperature and ambient temperature was assumed equal 300 K.

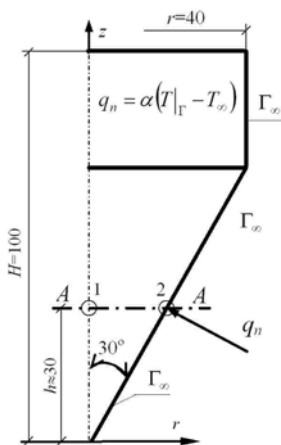


Fig. 7. Form and dimensions of the hardening object

The heating performed to the moment of cross maximal temperature 1500 K in environment of heat source (point 2, Fig. X). Provide this obtain requirements austenite zone in parts conic fang lathe. The temperature distributions after heating and obtained zone of austenite presented on the figure 8.

The cooling simulated by flux results from the difference of temperature among side surface and cooling medium (Newton condition). The temperature of cooling medium is equal 300 K. The coefficient of thermal conductivity was constant and was equal $\alpha^T=4000$ [W/(m²K)] (cooling in fluid layer [12]). The cooling performed to obtain by object ambient temperature, and

final of structures.

Obtained results of simulations were presented on the figures 8-10. The part of results (Fig. 10) along the radius (r) in cross section A-A and in distinguish points of cross sections (Fig. 7).

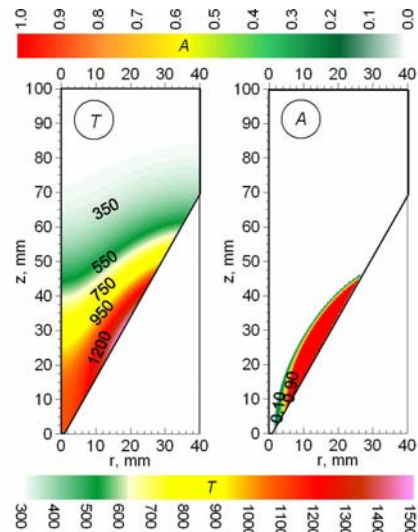


Fig. 8. Distributions: temperature a) and austenite b) after heating

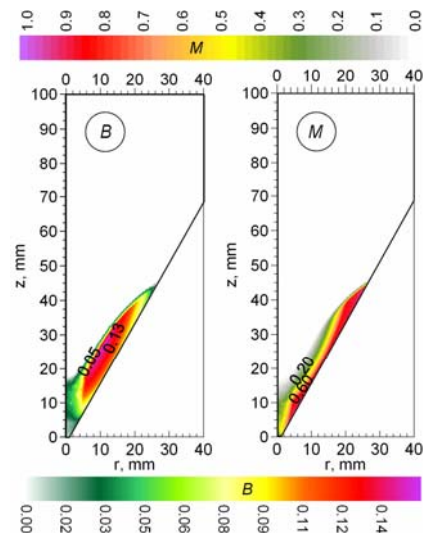


Fig. 9. Zones: bainite a) and martensite b) after quenching

5. Conclusions

As it has been already mentioned, using of CCT diagrams within the cooling rate ranges wherein three transformations are observed: pearlitic, bainitic and martensitic, guarantees more precise results. The results are shown in figures 8, 9 and 10. The results obtained with the application of CCT diagram are closer to the results of experimental research. The results of verification simulation of phase transformation kinetics (Fig. 6) prove that application of CCT diagrams enables good precise determination

of fractions and kinetics of newly-created phases depending on the cooling rate. Therefore for simulating phase transformations in the object undergoing hardening of the calculation example (fang lathe) a model based upon CCT diagrams was used (Fig. 3).

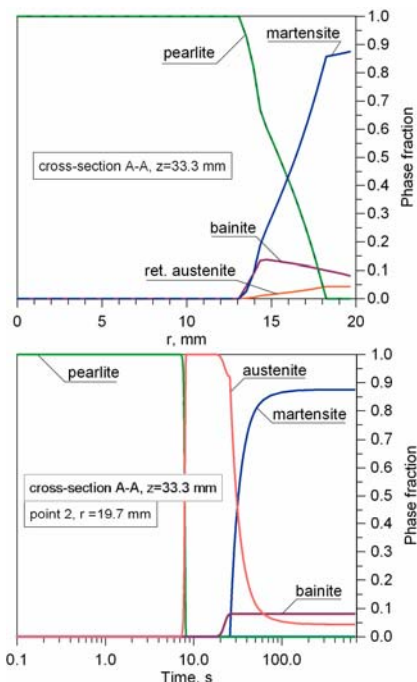


Fig. 10. Phase fractions along radius (cross section A-A) and their kinetics in point 2 (Fig. 7)

The simulations provide to very valuable distribution of temperature and good area of austenite deposition were obtained (Fig. 8). The hardened area after cooling appeared very beneficial, as well, which means that it is very well situated. The structure of the area after hardening is very good (certain fraction of bainite and significant fraction of martensite) (Fig. 9). In the hardened zone a small fraction of residual austenite (approximately 5%) was received. The point of the lathe was not hardened at all. It is very valuable from the practical point of view with respect to the purpose of such a machinery part.

Model numeryczny przewidywania mikrostruktury elementów stalowych obrabianych cieplnie

Streszczenie

Prezentowany w pracy model numeryczny procesu hartowania stali narzędziowej uwzględnia zjawiska cieplne i przemiany fazowe w stanie stałym. Algorytm numeryczny zjawisk cieplnych oparto na rozwiązaniu metodą elementów skończonych, w sformułowaniu Galernika, równania przewodzenia ciepła. W modelu przemian fazowych korzysta się z wykresów ciągłego nagrzewania (CTPa), oraz z wykresów ciągłego chłodzenia (CTPc) rozważanej stali. Ułamek fazy przemienionej (austenit) oraz ułamki ferrytu, perlitu lub bainitu wyznacza się formułami Johnsona-Mehla i Avramiego. Ułamek powstającego martenzytu wyznacza się wzorem Koistinen i Marburgera lub zmodyfikowanym wzorem Koistinen i Marburgera.

References

- [1] S-H. Kang, Y.T. Im, Three-dimensional thermo-elastic-plastic finite element modeling of quenching process of plain carbon steel in couole with phase transformation. *Journal of Materials Processing Technology* 192-193, (2007) 381-390.
- [2] A. Bokota, A. Kulawik, Model and numerical analysis of hardening process phenomena for medium-carbon steel, *Archives of Metallurgy and Materials Issue 2, vol. 52, (2007) 337-346.*
- [3] W.P Oliveira, M.A. Savi, P.M.C.L. Pacheco, L.F.G. Souza, Thermomechanical analysis of steel cylinders with diffusional and non-diffusional phase transformations. *Mechanics of Materials* 42 (2010) 31-43.
- [4] S.H. Kang, Y.T. Im, Thermo-elastic-plastic finite element analysis of quenching process of carbon steel. *International Journal of Mechanical Sciences* 49, (2007) 13-16.
- [5] A. Bokota, T. Domański, Numerical analysis of thermo-mechanical phenomena of hardening process of elements made of carbon steel C80U, *Archives of Metallurgy and Materials Issue 2, vol. 52, (2007) 277-288.*
- [6] E.P. Silva, P.M.C.L. Pacheco, M.A. Savi, On the thermo-mechanical coupling in austenite-martensite phase transformation related to the quenching process, *International Journal of Solids and Structures*, 41, (2004) 1139-1155.
- [7] D.Y. Ju, W.M. Zhang, Y. Zhang, Modeling and experimental verification of martensitic transformation plastic behavior in carbon steel for quenching process, *Material Science and Engineering A* 438-440, (2006) 246-250.
- [8] M. Pietrzyk, Through-process modelling of microstructure evolution in hot forming of steels, *Journal of Materials Technology*, 125-126, (2002) 53-62.
- [9] M. Białecki, Characteristic of steels, series F, tom I, Silesia Editor, (1987) 108-129, 155-179, (in polish).
- [10] K.J. Lee, Characteristics of heat generation during transformation in carbon steel. *Scripta Materialia* 40, (1999) 735-742.
- [11] L. Huiping, Z. Guoqun, N. Shanting, H. Chuanzhen, FEM simulation of quenching process and experimental verification of simulation results, *Material Science and Engineering A* 452-453, (2007) 705-714.
- [12] J. Jasiński, Influence of fluidized bed on diffusional processes of saturation of steel surface layer. *Seria: Inżynieria Materiałowa Nr 6, Editor WIPMiFS, Częstochowa (2003), (in polish).*